**Доклади на Българската академия на науките**
**Comptes rendus de l'Académie bulgare des Sciences**

*Tome 75, No 4, 2022*

*ENGINEERING SCIENCES*

*Computational physics*

# AN IMPROVED SEVENTH ORDER HERMITE WENO SCHEME FOR HYPERBOLIC CONSERVATION LAWS

**Yousef H. Zahran, Amr H. Abdalla**

*Received on October 19, 2020*
*Presented by Ch. Roumenin, Member of BAS, on December 21, 2021*

**Abstract**

A seventh order Hermite weighted essentially non-oscillatory (HWENO) scheme [1] has been used successfully to solve hyperbolic conservation laws. However, the scheme could not achieve the optimal order of accuracy at critical points. In this paper, we propose a new central seventh order HWENO scheme. It involves seventh order HWENO reconstruction [1] and the central-upwind flux [2,3]. For the ideal weights we used the central procedure presented in [4] and for nonlinear weights we extend the strategy proposed in [5,6]. For time integration, the seventh order linear strong-stability-preserving Runge–Kutta ($\ell SSPRK$) scheme is used. The resulting scheme combines the advantages of both the improved and Hermite central schemes, e.g., compactness, improving the convergence and accuracy at critical points, decreasing the dissipation near discontinuities especially for long time evolution problems; it is simple to implement and attains seventh order accuracy. Many numerical tests are presented to validate the performance of the proposed scheme.

**Key words:** conservation laws, Hermite WENO, $\ell SSPRK$, Euler equations

**1. Introduction.** WENO methods [7,8] are based on the essentially non-oscillatory (ENO) methods [9]. They use a nonlinear convex combination of all candidate stencils instead of the smoothest one in the ENO methods. They have the following advantages: high order accuracy in smooth regions and smooth extrema, unlike TVD schemes [10]; sharp and nonoscillatory shock transition.

DOI:10.7546/CRABS.2022.04.12

However, it is well known that WENO schemes are much more dissipative than central schemes. There are many techniques to decrease the numerical dissipation [5,11–14]. Borges et al. [11] introduced a new set of WENO weights which satisfy the necessary and sufficient conditions for optimal order at the critical points. The adaptive scheme [5] maintains the good shock-capturing properties of the classical WENO schemes and achieves very small numerical dissipation. However, this scheme is not valid at critical points, it increases numerical dissipation considerably. The main disadvantage of the classical WENO methods is that the wide stencil is not optimum either in terms of an accurate treatment of weak fluctuations, or concerning the imposition of boundary conditions. To overcome this problem, the stencil width should be reduced. The compactness of a numerical stencil has many advantages: firstly, for the same formal accuracy, compact stencils exhibit significantly more resolution by improving the dispersive and dissipative properties of the numerical schemes; secondly, boundary conditions are easier to deal with. In [15], fifth order HWENO schemes in which the function and its first derivative are evolved in time and used in the reconstruction, while only the function values are evolved and used in the original WENO schemes. The major advantage of HWENO schemes is their compactness. HWENO schemes have been improved by many authors e.g., [1,4,15–17]. In [1], a seventh order HWENO scheme is presented. Its advantages are that it is compact, more accurate and with high resolution. However, it fails to achieve the optimal order of accuracy at the critical points. In [4], a sixth order HWENO scheme was presented on three points stencil. It is an extension of the idea of Levy et al. [18]. The main advantage of this method is that the choice of the ideal weights has no effect on the accuracy and simplicity for computing the ideal weights. To fade the above schemes flaws and maintain their advantages, we propose here a new central scheme. It consists of the seventh order HWENO reconstructions, for ideal weights, we used the procedure presented in [4], for nonlinear weights, we extend the strategy presented in [5,6]. We use the central-upwind flux [2,3] which is simple, universal, efficient and can be used for problems with non-convex fluxes, the seventh order $\ell SSPRK$ for time integration is used. The resulting scheme combines the advantages of those schemes which are listed as follows: compactness, improving the convergence and accuracy at critical points as well as decreasing the numerical dissipation near discontinuities; this is due to the using of the new smoothness indicators; it lies upon a central and local WENO interpolation, it is more accurate and more efficient. The paper consists of four sections as follows. In Section 2 we review the HWENO reconstructions. In Section 3 we present the new central seventh order HWENO reconstruction. Section 4 presents the results of numerical examples of our method. Conclusions are presented in Section 5.

**2. Seventh order HWENO reconstruction.** Here we review the HWENO reconstruction to solve a scalar hyperbolic conservation law

$$u_t + [f(u)]_x = 0, \quad u(x,0) = u_0(x), \quad x \in (-\infty, \infty),\ t \in (0, \infty), \tag{2.1}$$

where $u(x,t)$ is a conserved quantity and $f(u)$ is the physical flux. Let $x_j = j\Delta x$, $x_{j\pm\frac{1}{2}} = x_j \pm \frac{1}{2}\Delta x$, $t^n = n\Delta t$, $u_j^n = u(x_j, t^n)$ and the cell $I_j = \left[x_{j-\frac{1}{2}}, x_{j+\frac{1}{2}}\right]$, where $\Delta x$ and $\Delta t$ are small spatial and time scales. Let $v = u_x$ and $g(u,v) = f'(u)u_x = f'(u)v$. Then from (2.1) and its spatial derivative we get

$$\left.\begin{aligned} u_t + [f(u)]_x &= 0, & u(x,0) &= u_0(x) \\ v_t + [g(u,v)]_x &= 0, & v(x,0) &= v_0(x) \end{aligned}\right\}. \tag{2.2}$$

Define the cell averages of $u$ and $v$ as

$$\overline{u}_j(t) = \frac{1}{\Delta x}\int_{I_j} u(x,t)\,\mathrm{d}x, \quad \overline{v}_j(t) = \frac{1}{\Delta x}\int_{I_j} v(x,t)\,\mathrm{d}x.$$

Equation (2.2) can be approximated by integrating (2.1) over $I_j$ to get the semi-discrete finite volume scheme

$$\left.\begin{aligned} \frac{\mathrm{d}}{\mathrm{d}t}u_j(t) &= -\frac{1}{\Delta x}\left\{F_{j+\frac{1}{2}} - F_{j-\frac{1}{2}}\right\} = L_j(u) \\ \frac{\mathrm{d}}{\mathrm{d}t}v_j(t) &= -\frac{1}{\Delta x}\left\{G_{j+\frac{1}{2}} - G_{j-\frac{1}{2}}\right\} = M_j(v) \end{aligned}\right\}, \tag{2.3}$$

where $F_{j+\frac{1}{2}}(G_{j+\frac{1}{2}})$ is the numerical flux $F(G)$ at $x_{j+\frac{1}{2}}$ and time $t$ as

$$\left.\begin{aligned} F_{j+\frac{1}{2}} &\approx \hat{F}_{j+\frac{1}{2}} = \hat{F}_{j+\frac{1}{2}}\left(u^L_{j+\frac{1}{2}}, u^R_{j+\frac{1}{2}}\right) \\ G_{j+\frac{1}{2}} &\approx \hat{G}_{j+\frac{1}{2}} = \hat{G}_{j+\frac{1}{2}}\left(u^L_{j+\frac{1}{2}}, v^L_{j+\frac{1}{2}}, u^R_{j+\frac{1}{2}}, v^R_{j+\frac{1}{2}}\right) \end{aligned}\right\}.$$

Here $u^{L,R}_{j+\frac{1}{2}}\left(v^{L,R}_{j+\frac{1}{2}}\right)$ are the numerical approximations to the functions $u(v)$ at the left and right of the interface $x_{j+\frac{1}{2}}$.

**3. The improved seventh order HWENO scheme.** Now, we construct the new central seventh order HWENO scheme. The implementation of the numerical scheme (2.3) is described as follows:

1. Reconstruction of $u^{L(R)}_{j+\frac{1}{2}}$ and $v^{L(R)}_{j+\frac{1}{2}}$.
2. Evaluation of the numerical fluxes.
3. The numerical solutions of (2.3) is advanced in time by using the seventh order ($\ell SSPRK$) [19].

***3.1. Reconstruction of $u_{j+\frac{1}{2}}^{L(R)}$ by seventh order HWENO method.*** Given the stencils

$$S_0 = \{x_{j-2}, x_{j-1}, x_j\}, \quad S_1 = \{x_{j-1}, x_j, x_{j+1}\}, \quad S_2 = \{x_j, x_{j+1}, x_{j+2}\},$$

and the central stencil $\tau = S_0 \cup S_1 \cup S_2$, we construct Hermite third degree polynomials $P_j(x)$ over $S_j$, $j = 0, 1, 2$, satisfying

$$\begin{aligned}
&\frac{1}{\Delta x}\int_{I_{j+i}} P_0(x)\,\mathrm{d}x = u_{j+i}, \quad i = -2,-1,0, \qquad \frac{1}{\Delta x}\int_{I_{j-1}} P_0'(x)\,\mathrm{d}x = v_{j-1},\\
&\frac{1}{\Delta x}\int_{I_{j+i}} P_1(x)\,\mathrm{d}x = u_{j+i}, \quad i = -1,0,1, \qquad \frac{1}{\Delta x}\int_{I_{j+1}} P_1'(x)\,\mathrm{d}x = v_{j+1}\\
&\frac{1}{\Delta x}\int_{I_{j+i}} P_2(x)\,\mathrm{d}x = u_{j+i}, \quad i = 0,1,2, \qquad \frac{1}{\Delta x}\int_{I_{j+1}} P_2'(x)\,\mathrm{d}x = v_{j+1}.
\end{aligned} \tag{3.1a}$$

Then we define a sixth degree polynomial $Q(x)$ over $\tau$

$$\begin{aligned}
&\frac{1}{\Delta x}\int_{I_{j+i}} Q(x)\,\mathrm{d}x = u_{j+i}, \qquad i = -2,-1,0,1,2,\\
&\frac{1}{\Delta x}\int_{I_{j+i}} Q_2'(x)\,\mathrm{d}x = v_{j+i}, \qquad i = -1,1.
\end{aligned} \tag{3.1b}$$

From (3.1a) and (3.1b) we get these polynomials at $x_{j+\frac{1}{2}}$

(3.2)

$$\left.\begin{aligned}
P_0(x_{j+\frac{1}{2}}) &= \tfrac{1}{12}(-5u_{j-2} - 14u_{j-1} + 31u_j - 18\Delta x v_{j-1})\\
P_1(x_{j+\frac{1}{2}}) &= \tfrac{1}{24}(-u_{j-1} + 8u_j + 17u_{j+1} - 6\Delta x v_{j+1})\\
P_2(x_{j+\frac{1}{2}}) &= \tfrac{1}{12}(u_j + 10u_{j+1} + u_{j+2} - 6\Delta x v_{j+1})\\
Q(x_{j+\frac{1}{2}}) &= \tfrac{1}{32000}(-319u_{j-2} - 5692u_{j-1} + 18150u_j + 19324u_{j+1} + 537u_{j+2}\\
&\quad - 7630\Delta x v_{j-1} - 7630\Delta x v_{j+1})
\end{aligned}\right\}.$$

To compute the ideal weights $d_k$, $k = 0, 1, 2$, we extend the principle of central WENO interpolation [4]. Firstly, we construct the central fourth polynomial $P_C(x)$ based on $\tau$ to satisfy the relation

$$Q(x_{j+\frac{1}{2}}) = \sum_{k\in\{0,1,2,C\}} d_k P_k(x_{j+\frac{1}{2}}), \quad d_k > 0, \qquad \sum_{k\in\{0,1,2,C\}} d_k = 1. \tag{3.3}$$

This polynomial is constructed in such a way that the convex combination (3.3) is 7-th order accurate in smooth regions. As noted in [4,18], the freedom in selecting these weights does not affect the properties of the numerical stencil; any symmetric choice in (3.3) produces the desired accuracy. Here we choose

$$d_0 = d_2 = \frac{1}{8}, \quad d_1 = \frac{1}{4}, \quad d_C = \frac{1}{2}. \tag{3.4}$$

Therefore, $P_C(x)$ becomes

$$P_C(x_{j+\frac{1}{2}}) = \frac{1}{d_C}\left[Q_(x_{j+\frac{1}{2}}) - d_0P_0(x_{j+\frac{1}{2}}) - d_1P_1(x_{j+\frac{1}{2}}) - d_2P_2(x_{j+\frac{1}{2}})\right],$$

$$\begin{aligned}(3.5)\quad P_C(x_{j+\frac{1}{2}}) &= \tfrac{1}{48000}(4043u_{j-2} - 2076u_{j-1} + 14450u_j + 30972u_{j+1}\\ &\quad + 611u_{j+2} - 4890\Delta x v_{j-1} - 10890\Delta x v_{j+1}).\end{aligned}$$

The smoothness indicators are written in the general form [8]

$$(3.6)\qquad \beta_j \equiv \sum_{k=1}^{3}\Delta x^{2k-1}\int_{x_{j-\frac{1}{2}}}^{x_{j+\frac{1}{2}}}\left(\frac{\mathrm{d}^k}{\mathrm{d}x^k}P_j(x)\right)^2\mathrm{d}x,\quad j=0,1,2,C.$$

The nonlinear weights $\omega_j$, $j=0,1,2,C$, are given by

$$(3.7)\qquad \omega_j = \frac{\alpha_j}{\sum\limits_{k=\{0,1,2,C\}}\alpha_k},\quad \text{where}\quad \alpha_k = \frac{d_k}{(\varepsilon+\beta_k)^2},\quad k=0,1,2,C,$$

where $\varepsilon$ is used to avoid the division by zero. The Taylor expansion of (3.6) gives

(3.8)

$$\left.\begin{aligned}
\beta_0 &= u_j'^2\Delta x^2 + \tfrac{13}{12}u_j''^2\Delta x^4 + \left(-\tfrac{1}{6}u_j'u_j^{(4)} - \tfrac{7}{72}u_j''u_j^{(3)}\right)\Delta x^5\\
&\quad + \left(\tfrac{781}{720}u_j'''^2 - \frac{65}{72}u_j''u_j^{(4)}\right)\Delta x^6 + \left(-\tfrac{17}{25}u_j'''u_j^{(4)} - \tfrac{7}{32}u_j'u_j^{(6)}\right)\Delta x^7 + o(\Delta x)^8,\\
\beta_1 &= u_j'^2\Delta x^2 + \left(\tfrac{13}{12}u_j''^2 - \tfrac{13}{500}u_j'u_j'''\right)\Delta x^4 - \tfrac{1}{12}u_j'u_j^{(4)}\Delta x^5\\
&\quad + \left(\tfrac{3139}{11520}u_j'''^2 + \tfrac{13}{72}u_j''u_j^{(4)}\right)\Delta x^6 + \left(\tfrac{11}{72}u_j'''u_j^{(4)} - \tfrac{171}{576}u_j'u_j^{(6)}\right)\Delta x^7 + o(\Delta x)^8,\\
\beta_2 &= u_j'^2\Delta x^2 + \left(\tfrac{13}{12}u_j''^2 + \tfrac{1}{12}u_j'u_j'''\right)\Delta x^4 + \left(-\tfrac{1}{2}u_j'u_j^{(4)} + \tfrac{1}{120}u_j''u_j'''\right)\Delta x^5\\
&\quad + \left(-\tfrac{9553}{4000}u_j'''^2 - 65u_j''u_j^{(4)} + \tfrac{1}{12}u_j'^2u_j^{(4)}\right)\Delta x^6\\
&\quad + \left(-\tfrac{879}{4000}u_j'''u^{(4)} + \tfrac{13}{16}u_j'u_j^{(6)}\right)\Delta x^7 + o(\Delta x)^8,\\
\beta_C &= u_j'^2\Delta x^2 + \left(\tfrac{13}{12}u_j''^2 - \tfrac{247}{6400}u_j'u_j'''\right)\Delta x^4\\
&\quad + \left(\tfrac{459}{25000}u_j'u_j^{(5)} + \tfrac{259}{1250}{}_ju_j'''^2 + \tfrac{43}{4800}u_j''u_j^{(4)}\right)\Delta x^6 + o(\Delta x)^8,
\end{aligned}\right\}.$$

The sufficient condition for $(2r-1)$-th order accuracy is given by [11,12]

$$(3.9)\qquad \omega_k = d_k + o(\Delta x^r).$$

From (3.8), the general form of $\beta_k$ can be written as

$$\beta_k = A(1+o(\Delta x)^2)$$

which results in

$$\omega_k = d_k + o(\Delta x^2)$$

which does not satisfy the sufficient conditions (3.9) for seventh order accuracy (from $2r-1=7$, we get $r=4$). Following the procedure in [5,6], we introduce the new weights

$$\omega_k^* = \frac{\alpha_k^*}{\sum\limits_{\ell\in\{0,1,2,C\}} \alpha_\ell^*}, \quad \alpha_k^* = d_k\left(A + \left[\frac{\tau_7}{\beta_k+\varepsilon}\right]^q\right),\ k=0,1,2,C \tag{3.10}$$

the parameter $A \gg 1$ and $\varepsilon = 10^{-40}$. Let the smoothness indicator $\tau_7$ be defined by

$$\tau_7 = \beta_Q - \frac{1}{6}[\beta_0 + 4\beta_1 + \beta_2]. \tag{3.11}$$

Here $\beta_Q$ is the smoothness indicator of $Q(x)$ and its Taylor expansion is given by

$$\begin{aligned}\beta_Q = {} & u_j'^2\Delta x^2 + \left(\tfrac{13}{12}u_j''^2 - \tfrac{1}{150}u_j'u_j'''\right)\Delta x^4 + \left(\tfrac{43}{240}u_j'u_j^{(4)} - \tfrac{4}{315}u_j''u_j'''\right)\Delta x^5 \\ & + \left(\tfrac{757}{90000}u_j'''^2 - \tfrac{77}{60000}u_j'u_j^{(5)} - \tfrac{403}{4500}u_j''u_j^{(4)}\right)\Delta x^6 \\ & + \left(-\tfrac{1333}{160000}u_j'u^{(6)} - \tfrac{559}{28800}u_j'''u_j^{(4)}\right)\Delta x^7 + o(\Delta x)^8.\end{aligned} \tag{3.12}$$

Therefore the truncation errors of $\tau_7$ are given by

$$\tau_7 = \begin{cases} 0.02u'u^{(4)}\Delta x^5 + o(\Delta x)^6 & u' \neq 0, \\ 6.02u''u^{(4)}\Delta x^6 + o(\Delta x)^8 & u'=0,\ u''\neq 0, \\ 4.79u'u^{(4)}\Delta x^8 + o(\Delta x)^6 & u'=u''=0,\ u'''\neq 0. \end{cases} \tag{3.13}$$

From (3.11)–(3.13) we get

$$\omega^* - d_k = \begin{cases} o(\Delta x)^{3q} & u'\neq 0, \\ o(\Delta x)^{2q} & u'=0,\ u''\neq 0, \\ o(\Delta x)^{2q} & u'=u''=0,\ u'''\neq 0, \end{cases} \qquad k=0,1,2,C. \tag{3.14}$$

Therefore, for choosing $q=2$, the scheme achieves seventh order accuracy in smooth regions as well as at the critical points. The final seventh order HWENO reconstruction is then given by

$$u_{j+\frac{1}{2}}^L = \sum_{k=\{0,1,2,C\}} \omega_k^* P_k(x_{j+\frac{1}{2}}). \tag{3.15}$$

The reconstruction of $u_{j+\frac{1}{2}}^R$ is mirror symmetric with respect to $x_j$ of the last procedure.

***3.2. Reconstruction of $v_{j+\frac{1}{2}}^{L(R)}$.***

To reconstruct $v_{j+\frac{1}{2}}^{L(R)}$ we proceed as in the last section and get

$$\omega_k^* - d_k = \begin{cases} o(\Delta x)^{4q} & u'' \neq 0, \\ o(\Delta x)^{2q} & u'' = 0,\ u''' \neq 0, \\ o(\Delta x)^{2q} & u'' = u''' = 0, \end{cases} \quad k = 0, 1, 2, C. \tag{3.16}$$

Therefore, for $q = 2$, the scheme achieves seventh order accuracy in smooth regions as well as at the critical points.

The seventh order HWENO reconstruction is then given by

$$v_{j+\frac{1}{2}}^{L} = \sum_{k=\{0,1,2,C\}} \omega_k^* P_k'(x_{j+\frac{1}{2}}). \tag{3.17}$$

**Remark 1.** For the numerical flux, we use the central-upwind flux [2, 3] which is simple, universal, efficient and can be used for problems with non-convex fluxes.

**Remark 2.** For systems cases, to avoid oscillations, the reconstruction is carried out in characteristic variables rather than the conserved variables and (3.15) and (3.17) are applied to each characteristic field.

***3.3. Time discretization.*** The semi-discrete scheme (2.3) is a system of ODEs, which can be solved by any stable ODE solver. Here we use $\ell SSPRK$ $(m, m-1)$, i.e., $m$-stage and $(m-1)$-th order method [19]. This method is used to solve a system of ODEs

$$\frac{\mathrm{d}u}{\mathrm{d}t} = L(u), \tag{3.18}$$

where $L(u)$ is an approximation to the derivative $(-f(u)_x)$ in (2.1). This $\ell SSPRK$ $(m, m-1)$ method takes the form:

$$\begin{aligned} &u^{(0)} = u^n, \\ &u^{(i)} = u^{(i-1)} + \tfrac{1}{2}\Delta t L(u^{(i-1)}), \quad i = 1, \ldots, m-1, \\ &u^{n+1} = u^{(m)} = \sum_{k=0}^{m-2} \alpha_{m,k} u^{(k)} + \alpha_{m,m-1}\left(u^{(m-1)} + \tfrac{1}{2}\Delta t L(u^{(m-1)})\right). \end{aligned} \tag{3.19}$$

Here we use the seventh order ($m = 8$). The stability condition for the schemes is CFL $\leq 1$, where CFL is the Courant number.

**4. Numerical experiments.** Here we compare the schemes HWENO7 in [1] and IHWENO7 presented here. Here, we take CFL $= 0.4$ and $\varepsilon = 10^{-40}$.

***Accuracy test at the critical points.*** Here, we test the accuracy of the proposed scheme at the critical points. Let us consider the test functions $g_n(x) = x^{n+1}$, $n \geq 1$ [20] with $n$-th order critical point at $x = 0$. Table 1 shows the $L^1$ errors and convergence rates of the schemes at the critical point $x = 0$. From Table 1 we note that:

T a b l e 1

Convergence study of the function $g_1(x)$ (left) and $g_2(x)$ (right) at critical point $x = 0$

| $N$ | HWENO7 | | IHWENO7 | | $N$ | HWENO7 | | IHWENO7 | |
|---|---|---|---|---|---|---|---|---|---|
| | $L^1$ error | $L^1$ order | $L^1$ error | $L^1$ order | | $L^1$ error | $L^1$ order | $L^1$ error | $L^1$ order |
| 200 | 6.22E−11 | | 1.96E−14 | | 200 | $5.66E{-}7$ | | $1.81E{-}11$ | |
| 400 | 3.86E−12 | 4.01 | 1.46E−16 | 7.07 | 400 | $7.02E{-}8$ | 3.01 | $1.75E{-}13$ | 6.69 |
| 800 | 2.41E−13 | 4.00 | 1.08E−18 | 7.08 | 800 | $8.34E{-}9$ | 3.08 | $1.71E{-}15$ | 6.67 |
| 1600 | 1.51E−14 | 3.99 | 7.83E−21 | 7.11 | 1600 | $1.01E{-}9$ | 3.04 | $1.66E{-}17$ | 6.72 |
| 3200 | 9.37E−16 | 4.01 | 5.79E−23 | 7.08 | 3200 | $1.19E{-}10$ | 3.09 | $1.61E{-}19$ | 6.68 |

1. For $g_1(x)$, IHWENO7 scheme achieves the optimal seventh order while HWENO7 scheme attains only fourth order.

2. For $g_2(x)$, IHWENO7 scheme recovers (approximately) the optimal seventh order accuracy while HWENO7 scheme attains third order only.

**Example 1.** We consider equation (2.1) with the initial condition

$$u(x,0) = \begin{cases} \frac{1}{6}[G(x,z-\delta) + G(x,z+\delta) + 4G(x,z)], & -0.8 \le x \le -0.6, \\ 1, & -0.4 \le x \le -0.2, \\ 1 - |10(x-0.1)| & 0 \le x \le 0.2, \\ \frac{1}{6}[F(x,a-\delta) + F(x,a+\delta) + 4F(x,a)], & 0.4 \le x \le 0.6 \\ 0, & \text{otherwise}, \end{cases} \tag{4.1}$$

where $G(x,z) = \exp(-\beta(x-z)^2)$, $F(x,a) = \max\{1-\alpha^2(x-a)^2, 0\}^{1/2}$, $a = 0.5$, $z = -0.7$, $\delta = 0.005$, $\alpha = 10$ and $\beta = (\log 2)/36\delta^2$ with periodic boundary condition on $[-1,1]$. We compute the numerical solutions at $t = 20$ and very long time $t = 2000$ with 200 cells. Figure 1 shows the results with IHWENO7 scheme. The exact solution is shown by full line and the numerical solution is shown by symbols. Comparing the results in Fig. 1 and the results in [7,17], we notice that the accuracy of IHWENO7 is overall higher than that of the other methods. The

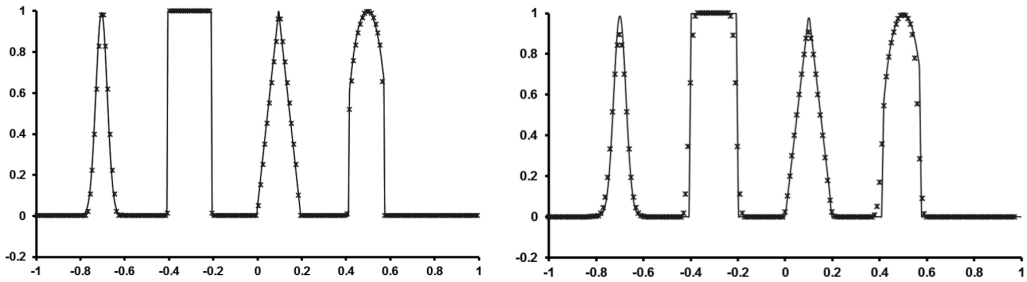


Fig. 1. Solution of Example 1 using IHWENO7 scheme at $t = 20$ (left) and at $t = 2000$ (right)

numerical results obtained by IHWENO7 scheme are almost indistinguishable from the exact solution. For $t = 2000$, we compare the results in Fig. 1 and the results in [1] and we observe that the results produced by IHWENO7 are superior to those obtained with all the others.

**Example 2** (The Lax problem)**.** The Euler equations of gas dynamics is given by

$$U_t + F(U)_x = 0, \tag{4.2}$$

where $U = (\rho, \rho u, E)^T$ and $F(U) = (\rho u, \rho u^2 + P, u(E + P))^T$. $\rho$ is the density, $u$ is the velocity, $P$ is the pressure, $E = \rho u^2/2 + P/(\gamma - 1)$ is the total energy, and $\gamma$ is the ratio of specific heats, taken as 1.4 here. Lax problem is equation (4.2) with initial conditions

(4.3)

$$(\rho_L, u_L, E_L)=(0.445, 0.311, 8.928) \text{ and } (\rho_R, u_R, E_R)=(0.5, 0.0, 1.4275),\ x \in [0, 1]$$

separated by a discontinuity at $x = 0.5$. Figure 2 shows the numerical results of IHWENO scheme at $t = 0.16$ with 100 cells. Comparing the results with [4,5], we see that IHWENO scheme is more accurate and efficient. We note that the adaptive scheme [5] and Capdeville scheme [4] produce oscillations near discontinuities.

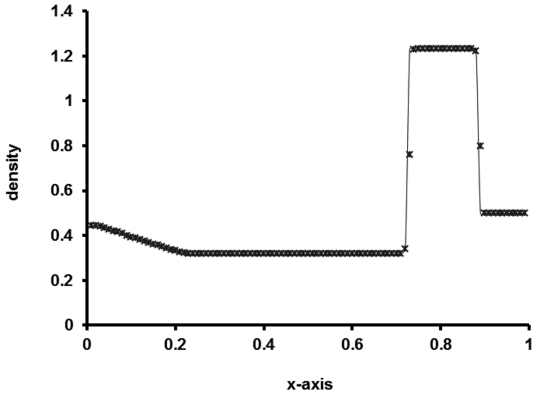


Fig. 2. Solution of Example 2

**Example 3** (The Shock-turbulence interaction problem)**.** To see the advantages of our method, we solve a problem with a rich smooth structure and a shock wave. It is equation (4.2) with a moving Mach = 3 shock interacting with sine waves in density, i.e., initially

$$\begin{aligned} &(\rho_L, u_L, P_L) = (3.857143, 2.629369, 10.3333) \qquad \text{for} \quad x < -4, \\ &(\rho_R, u_R, P_R) = (1 + 0.2 \sin 5x, 0, 1) \qquad \text{for} \quad x > -4. \end{aligned} \tag{4.4}$$

This flow contains physical oscillations which have to be resolved by the numerical method. Figure 3 shows the density computed by the IHWENO scheme at $t =$

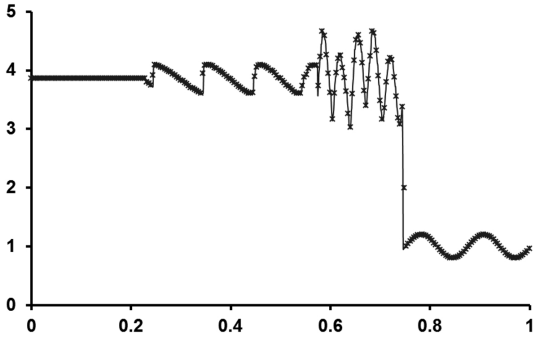

Fig. 3. Solution of Example 3

1.8 with 200 grid points. Comparing the results with [1,5] and [11,16,17] with 300 grids, we observe that our scheme is more accurate and more efficient than all the schemes since here we use 200 cells only.

**5. Conclusions.** In this paper, we propose a new central seventh order HWENO scheme. It consists of seventh order HWENO reconstruction [1] and the central-upwind flux [2,3]. The ideal weights are computed by using the central procedure [4] and the nonlinear weights are computed using the strategy in [5,6]. We used ($\ell SSPRK$) for time integration. The new scheme has the following advantages: compactness, improving the convergence and accuracy at critical points, decreasing the dissipation near discontinuities; it is simple to implement. Many numerical examples are solved to validate the performance of the new scheme. In the future we plan to use the present scheme for balance laws, multidimensional computations and unstructured meshes.

## REFERENCES

[1] Zahran Y. H., A. H. Abdalla (2016) Seventh order Hermite WENO scheme for hyperbolic conservation laws, J. Comput. Fluids, **131**, 66–80.

[2] Kurganov A., S. Noelle, G. Petrova (2001) Semi-discrete central-upwind schemes for hyperbolic conservation laws and Hamilton–Jacobi equations, SIAM. J. Sci. Comp., **23**, 707–740.

[3] Kurganov A., G. Petrova, B. Popov (2007) Adaptive semi-discrete central-upwind schemes for non-convex hyperbolic conservation laws, SIAM J. Sci. Comput., **29**, 2381–2401.

[4] Capdeville G. (2008) A Hermite upwind WENO scheme for solving hyperbolic conservation laws, J. Comput. Phys., **227**, 2430–2454.

[5] Hu X. Y., Q. Wang, N. A. Adams (2010) An adaptive central-upwind weighted essentially non-oscillatory scheme, J. Comp. Phys., **229**, 8952–8965.

[6] Sun Z., L. Luo, Y. Ren, S. Zhang (2014) A sixth order hybrid finite difference scheme based on the minimized dispersion and controllable dissipation technique, J. Comp. Phys., **270**, 238–254.

[7] Balsara D. S., C. W. Shu (2000) Monotonicity preserving weighted essentially non-oscillatory schemes with increasingly high order of accuracy, J. Comput. Phys., **160**, 405–452.
[8] Jiang G. S., C. W. Shu (1996) Efficient implementation of weighted ENO schemes, J. Comp. Phys., **126**, 202–228.
[9] Harten A., B. Enqueist, S. Osher, S. R. Chakravarthy (1987) Uniformly high order accurate essentially non oscillatory schemes, J. Comput. Phys., **71**, 231–303.
[10] Harten A. (1983) High resolution schemes for hyperbolic conservation laws, J. Comput.Phys., **49**, 357–393.
[11] Borges R., M. Carmona, B. Costa, W. Sun Don (2008) An improved weighted essentially non-oscillatory scheme for hyperbolic conservation laws, J. Comput. Phys., **227**, 3191–3211.
[12] Henrick K., T. D. Aslam, J. M. Powers (2005) Mapped weighted essentially non-oscillatory schemes: achieving optimal order near critical points, J. Comput. Phys., **207**, 542–567.
[13] Zahran Y. H. (2011) Very high order improved WENO scheme for hyperbolic conservation laws, C. R. Acad. Bulg. Sci., **64**(10), 1393–1402.
[14] Zahran Y. H., A. H. Abdalla (2018) A seventh order central HWENO scheme on staggered meshes for conservation laws, C. R. Acad. Bulg. Sci., **71**(12), 1603–1614.
[15] Qiu J., C.-W. Shu (2003) Hermite WENO schemes and their application as limiters for Runge–Kutta discontinuous Galerkin method: one-dimension case, J. Comput. Phys., **193**, 115–135.
[16] Liu H., J. Qiu (2015) Finite difference Hermite WENO schemes for conservation laws, J. Sci. Comput., **63**, 548–572.
[17] Liu H., J. Qiu (2015) Finite difference Hermite WENO schemes for conservation laws. II: An alternative approach, J. Sci. Comput., **66**, 598–624.
[18] Levy D., G. Pupo, G. Russo (2000) Compact central WENO schemes for multidimensional conservation laws, SIAM J. Sci. Comput., **22**, 656–672.
[19] Gottlieb S. (2005) On high order strong stability preserving Runge–Kutta and multistep time discretizations, J. Sci. Comput., **25**(1), 105–128.
[20] Wang B. S., P. Li, Z. Gao, W. Don (2018) An improved fifth order alternative WENO-Z finite difference scheme for hyperbolic conservation laws, J. Comput. Phys., **374**, 469–477.

*Physics and Mathematics Department*
*Faculty of Engineering*
*Port Said University*
*Port Said, Egypt*
*e-mails*: dryhhz@yahoo.com
amr.hassan1@hotmail.com